Analysis and Modeling of Human Impedance Properties for Designing a Human-Machine Control System

Yoshiyuki TANAKA   Teruyuki ONISHI   Toshio TSUJI
Naoki YAMADA   Yuusaku TAKEDA   Ichiro MASAMORI

Abstract— A human can control dynamic properties of his/her own body naturally and effectively according to tasks by utilizing the perceived information of environmental characteristics. If dynamic properties of human movements depending on environmental characteristics can be described quantitatively, there would be expected to design and develop a novel human-machine system in which an operator can manipulate more comfortably. This paper discusses a design methodology of human-machine systems integrating human motor characteristics. A vehicle interface system manipulated by the foot is focused on, and mechanical impedance properties of human lower extremities during maintained leg posture are investigated according to the leg posture and the foot force.

I. INTRODUCTION

A human adjusts his/her posture and force to realize skillful motions according to a target task. For example, when a driver tries to slow down the speed of an automobile without giving unpleasant inertial force for a fellow passenger, he would step on the brake gradually with regulating his foot force through controlling muscle activities in his lower limbs. Like in such a task with the physical interaction between a human operator and an interface of a machine, a human regulates dynamic properties of the limbs based on the external and/or internal information obtained from sensory receptors so that he/she can manipulate the machine skillfully. If human dynamic properties changing in the task can be quantitatively described, it would be useful to design and develop a novel human-machine system considering human sensory-motor characteristics so that an operator can manipulate a machine comfortably.

Based on such an assertion, Tanaka and Tsuji et al. [1] developed a human force manipulability by combining robotic manipulability with human joint-torque characteristics. Their method can evaluate and visualize the spatial characteristics of human force capability of the limbs for the measured limb's posture. Then, they have applied to the layout design of driving interfaces of an automobile [2]. However, their method cannot deal with dynamic properties of human movements, such as compliance and stiffness of motions.

Y. Tanaka, T. Onishi, and T. Tsuji are with Graduate School of Engineering, Hiroshima University, Higashi-hiroshima, JAPAN, {ytanaka, tsuji}@bsys.hiroshima-u.ac.jp

N. Yamada, Y. Takeda, and I. Masamori are with Mazda Motor Corporation, Hiroshima, JAPAN

Dynamic properties of human movements can be often expressed with the mechanical impedance parameters, i.e., stiffness, viscosity, and inertia, and many experimental studies on human impedance of the limbs have been reported. For example, Mussa-Ivaldi et al. [3] pioneered the measurement of human hand impedance and examining hand stiffness in a stable arm posture. They found that hand stiffness strongly depends on arm posture. Dolan et al. [4] and Tsuji et al. [5], [6] also showed that human hand viscoelasticity is widely affected by muscle activation level during isometric contraction. These experimental studies reveal that a human can control his/her impedance by regulating limb's posture and/or muscle contraction level during multi-joint movements.

On the other hand, Park and Sheridan [7] measured end-point stiffness of the lower limb in the process of evaluating a braking system from the viewpoint of pedaling motion of a human driver, in which a subject lay on the horizontal plane to eliminate the effect of gravity and his ankle joint was fixed. However, they did not consider viscosity and inertia of the lower limbs, and did not aim to design a control system considering human impedance properties.

Many methods have been proposed for designing and controlling a human-machine system constructed with an impedance-controlled robot [8] since the overall system can be described by the impedance property [9]–[14]. Those studies can be classified into two types according to whether the human impedance property is constant during operation [9], [11], [13], or variable [10], [12], [14]. No detailed discussion has addressed how a machine adapts its dynamics for human impedance properties that would widely change depending on human posture and muscle activations during operations.

The present paper aims to integrate such variable human impedance properties into a human-machine control system as shown in Fig. 1. A machine grasps human impedance
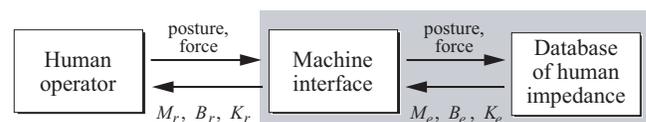

Fig. 1.   Conceptual block diagram of the proposed human-machine system.

(M_e, B_e, K_e) from the database with measured human posture and operational force, and regulates its mechanical

impedance (M_r, B_r, K_r) according to human movements.

In the rest part of this paper, a vehicle interface system manipulated by the foot, such as a brake pedal and a gas pedal, is focused on as an example of a human-machine system. Section II explains a method and an experimental apparatus using robotic devices for measuring human impedance of the lower limbs, and Section III describes measured human impedance properties depending on leg postures and foot forces with consideration of ankle joint motion. Finally, a designed human-machine control system is discussed by using the developed experimental system in Section IV.

II. HUMAN IMPEDANCE MEASUREMENT

A. A method

Let us consider multi-joint movements by the human lower extremity with n degree-of-freedom in the l-dimensional task space. When the subject's end-point is displaced from its equilibrium by a small disturbance with a short duration as shown in Fig. 2, dynamic characteristics of the end-point during maintained leg posture $\theta(t) \in \Re^n$ can be expressed with an impedance model [5][6] as

$$M_e \ddot{X}_e(t) + B_e \dot{X}_e(t) + K_e(X_e(t) - X_v(t)) \qquad (1)$$
$$+ g_x(\theta(t)) = -F_e(t),$$

where $F_e(t) \in \Re^l$ denotes the restoring force of the lower extremity applied to the environment; $X_e(t) \in \Re^l$ the end-point position; $X_v(t) \in \Re^l$ the virtual trajectory [3]; $g_x(\theta(t)) \in \Re^l$ the gravity term of the lower extremity expressed at the end-point; and M_e, B_e, and $K_e \in \Re^{l \times l}$ represent the inertia, viscosity and stiffness matrices at the end-point, respectively.

Assuming that $X_v(t)$ and $g_x(\theta(t))$ are constant for the applied external disturbance with short displacement, the following dynamic equation of the lower limb at the end-point can be derived from (2):

$$M_e d\ddot{X}(t) + B_e d\dot{X}(t) + K_e dX(t) = -dF(t), \qquad (2)$$

where $dX(t) = X_e(t) - X_e(t_0)$, $dF(t) = F_e(t) - F_e(t_0)$, and t_0 denotes the time when the disturbance is applied to the end-point. In this model, the impedance matrices can be estimated from the measured position $X_e(t)$ and force $F_e(t)$, induced by the external disturbance, with the least squares method.

B. Experimental apparatus

Fig. 3 shows an overview of the experimental system developed in this paper for measuring human impedance properties of the lower extremities. The system is composed of a linear motor table with one degree of freedom (NSK, LTD., encoder resolution: 1 [μm], maximum thrust: 400 [N]) as a robotic device, a computer for the robot control, and a visual feedback display to provide the experimental information to a subject.

A step and a six-axis force/torque sensor (BL Autotec Co.Ltd., resolution ability: force x axis, y axis: 25×10^{-3} [N], z axis: 75×10^{-2} [N], torque: 150×10^{-3} [Nm])
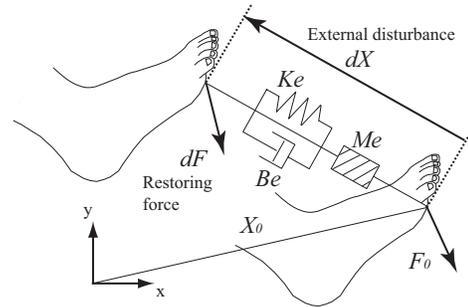

Fig. 2. Schematic description of human impedance measurements.
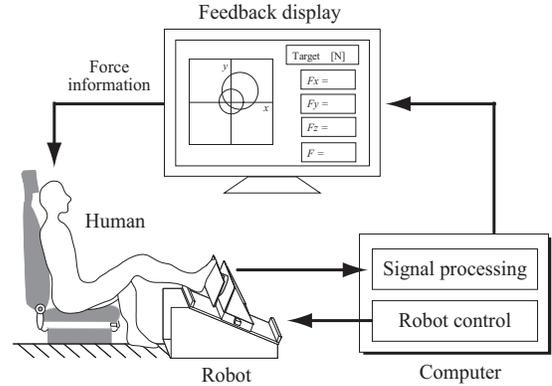

Fig. 3. An overview of the developed experimental system.

are attached to the moving part of the robot to measure the applied force F_e imposed by a human operator. The position is measured by encoder built into the motor table. The display feeds back the magnitude and direction of F_e by the size and center of a circle in real-time.

Mechanical impedance properties of a known spring-mass system were measured to validate performance of the experimental system, where the specified values of spring stiffness were 768, 1373, 1722, 2788 [N/m] and inertia of masses were 1.222, 2.444, 3.666, 4.888 [kg]. Fig. 4 shows an example of the measured signals for estimating mechanical impedance properties. The panels (a), (b), and (c) express time histories of the displacement of an end-point $dX(t)$, velocity $d\dot{X}(t)$, and acceleration $d\ddot{X}(t)$ caused by external disturbance in the order from the top. The solid line in the bottom panel (d) represents measured force together with estimated force (broken line) calculated from Eq.(2) with measured signals and estimated impedance parameters. It can be said that the experimental system accurately estimates mechanical impedance properties since the solid line almost coincides with the broken one. The standard deviations of estimated errors for stiffness and inertia were less than 77 [N/m], 0.18 [kg], respectively, within the specified conditions.

III. HUMAN IMPEDANCE PROPERTIES OF THE LOWER EXTREMITIES

A human subject has a seat set in front of the experimental system and his right foot is fixed on the moving part of
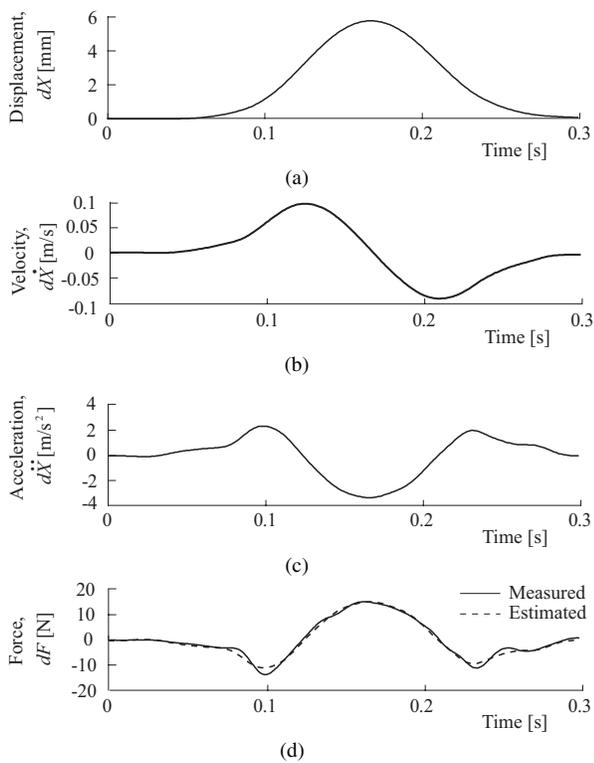
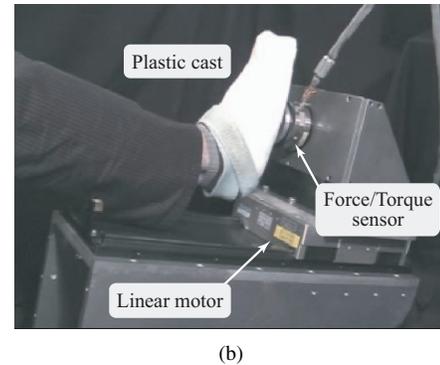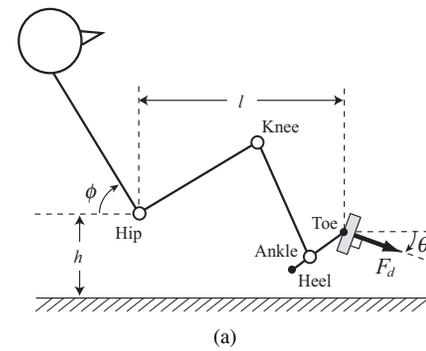Fig. 4. An example of measured signals during impedance measurements.

Fig. 5. Experimental condition for measuring human leg impedance.
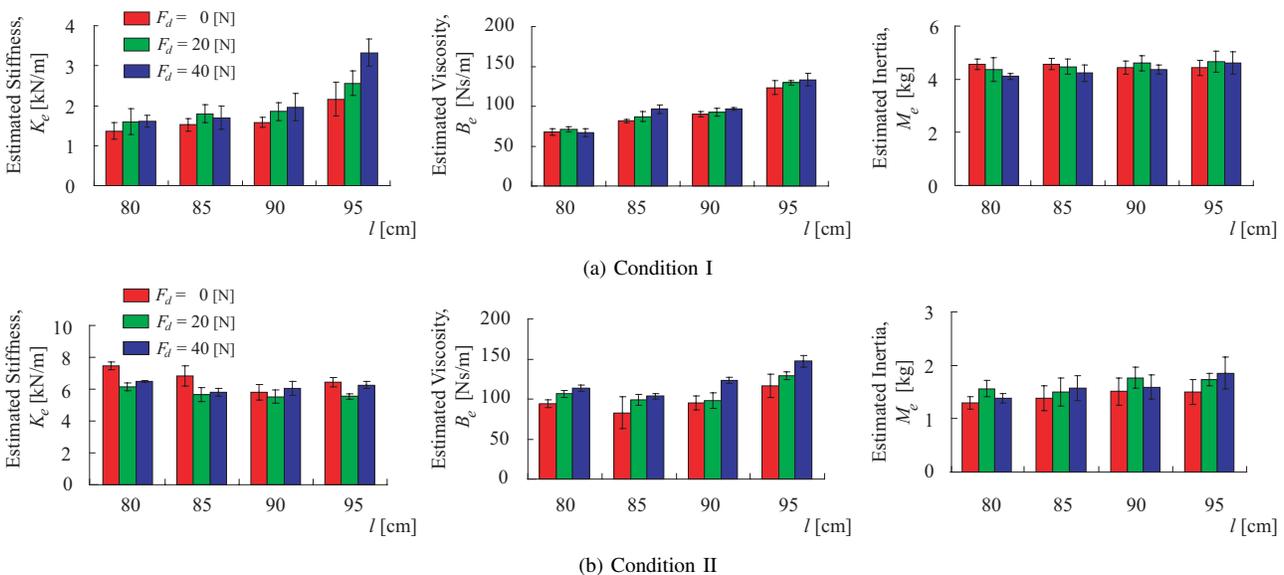

Fig. 6. Typical results of human leg impedance depending on the leg posture and foot force (Subject A).

the motor table by the plastic cast as shown in Fig. 5. The human lower extremity is expressed by a serial link with three rotational joints. During impedance measurements, he is asked to generate the specified end-point force with maintaining his leg posture by using the biofeedback display.

Experimental conditions were set as the distance l = 80, 85, 90, 95 [cm] and the target force F_d = 0, 20, 40 [N] under h = 15 [cm], ϕ = 75 [deg.] and θ = 22 [deg.]. Since the heel

conditions would much affect pedaling operations, a set of measuring experiments were carried out for the two cases where the heel is in contact with the ground (Condition I) or not (Condition II). Three healthy subjects (male university students) participated in the experiment.

Figure 6 shows the measured human leg impedance for Subject A in Condition I and II, where stiffness, viscosity, inertia depending on the distance l and the target force F_d are

TABLE I

MEASURED HUMAN LEG IMPEDANCE PROPERTIES FOR ALL SUBJECTS UNDER THE TWO CONDITIONS.

(a) Condition I

Subject A	Force, F_d [N]	Distance, l [cm]			
		80	85	90	95
Stiffness [N/m]	0	1365.2 ± 205.6	1524.6 ± 157.2	1584.0 ± 122.3	2165.8 ± 430.9
	20	1597.0 ± 324.4	1799.9 ± 231.3	1853.8 ± 225.4	2562.4 ± 308.7
	40	1609.4 ± 149.2	1697.3 ± 286.2	1962.5 ± 341.4	3327.5 ± 336.1
Viscosity [Ns/m]	0	67.77 ± 4.12	81.58 ± 1.95	90.45 ± 3.34	123.21 ± 8.63
	20	71.04 ± 3.23	87.07 ± 6.32	92.42 ± 4.99	129.51 ± 2.77
	40	66.74 ± 4.87	96.38 ± 5.29	96.59 ± 1.88	133.26 ± 7.89
Inertia [kg]	0	4.56 ± 0.19	4.56 ± 0.21	4.43 ± 0.25	4.43 ± 0.29
	20	4.36 ± 0.44	4.47 ± 0.30	4.60 ± 0.29	4.66 ± 0.40
	40	4.11 ± 0.11	4.23 ± 0.30	4.38 ± 0.17	4.61 ± 0.42

Subject B	Force, F_d [N]	Distance, l [cm]			
		80	85	90	95
Stiffness [N/m]	0	2854.4 ± 506.1	2580.9 ± 591.1	3227.2 ± 164.9	3907.0 ± 344.3
	20	3268.2 ± 642.7	3684.4 ± 484.3	3503.8 ± 121.3	4539.0 ± 110.3
	40	3529.0 ± 872.7	3678.1 ± 373.8	4989.5 ± 566.0	5043.4 ± 537.4
Viscosity [Ns/m]	0	130.12 ± 10.44	142.41 ± 10.20	142.23 ± 4.29	167.83 ± 8.66
	20	138.13 ± 13.54	143.76 ± 5.67	157.64 ± 5.60	182.30 ± 36.34
	40	120.48 ± 12.35	138.53 ± 20.51	143.90 ± 9.58	209.40 ± 35.80
Inertia [kg]	0	4.77 ± 0.46	4.41 ± 0.45	4.84 ± 0.11	3.56 ± 0.17
	20	4.71 ± 0.37	4.77 ± 0.59	5.14 ± 0.33	3.93 ± 0.54
	40	4.72 ± 0.63	4.63 ± 0.42	4.61 ± 0.42	3.91 ± 0.51

Subject C	Force, F_d [N]	Distance, l [cm]			
		80	85	90	95
Stiffness [N/m]	0	1604.6 ± 466.0	2475.9 ± 572.6	2973.1 ± 424.5	4874.5 ± 1199.6
	20	2168.4 ± 512.7	2449.4 ± 658.0	3543.3 ± 502.1	4595.8 ± 334.8
	40	2380.4 ± 948.1	3348.7 ± 1000.1	3968.1 ± 427.8	5675.1 ± 748.5
Viscosity [Ns/m]	0	99.91 ± 16.16	106.38 ± 17.00	109.49 ± 21.56	131.44 ± 11.94
	20	96.00 ± 14.55	105.80 ± 24.88	122.67 ± 13.78	128.51 ± 9.21
	40	104.60 ± 15.60	135.30 ± 17.73	149.65 ± 27.25	182.50 ± 19.27
Inertia [kg]	0	4.69 ± 0.82	4.68 ± 0.71	4.66 ± 1.14	3.91 ± 0.74
	20	4.55 ± 0.63	4.66 ± 0.34	4.27 ± 0.37	4.25 ± 0.65
	40	4.42 ± 0.73	4.65 ± 0.63	4.19 ± 0.48	4.01 ± 0.56

(b) Condition II

Subject A	Force, F_d [N]	Distance, l [cm]			
		80	85	90	95
Stiffness [N/m]	0	7478.1 ± 250.0*	6834.6 ± 618.6*	5806.8 ± 501.6*	6446.9 ± 306.2*
	20	6149.7 ± 230.7*	5640.0 ± 440.6*	5536.5 ± 396.4*	5541.3 ± 189.6*
	40	6503.8 ± 44.8*	5802.7 ± 227.0*	6060.1 ± 442.3*	6261.3 ± 215.6*
Viscosity [Ns/m]	0	93.86 ± 4.87*	82.97 ± 19.70	95.45 ± 8.85	116.34 ± 14.46
	20	106.32 ± 4.04*	99.30 ± 6.88*	98.51 ± 9.68	129.07 ± 5.05
	40	113.56 ± 4.22*	103.61 ± 3.38*	123.43 ± 4.06*	147.31 ± 7.27*
Inertia [kg]	0	1.29 ± 0.12*	1.38 ± 0.23*	1.51 ± 0.25*	1.50 ± 0.23*
	20	1.56 ± 0.16*	1.51 ± 0.26*	1.77 ± 0.20*	1.73 ± 0.11*
	40	1.39 ± 0.09*	1.57 ± 0.24*	1.59 ± 0.22*	1.85 ± 0.30*

Subject B	Force, F_d [N]	Distance, l [cm]			
		80	85	90	95
Stiffness [N/m]	0	13489.4 ± 1605.2*	9424.2 ± 428.2*	9350.4 ± 635.0*	8387.0 ± 897.7*
	20	10846.6 ± 746.7*	9997.4 ± 688.8*	9506.2 ± 598.1*	8514.6 ± 857.1*
	40	9594.4 ± 697.6*	9964.1 ± 892.9*	7448.5 ± 649.4*	9464.4 ± 394.2*
Viscosity [Ns/m]	0	177.48 ± 42.74*	141.85 ± 5.96	157.81 ± 15.76	156.89 ± 26.74
	20	150.46 ± 6.81	139.26 ± 12.31	159.24 ± 18.10	144.10 ± 25.69
	40	154.87 ± 6.18*	159.60 ± 10.96	155.11 ± 6.95	153.71 ± 14.66
Inertia [kg]	0	2.12 ± 0.36*	1.65 ± 0.15*	1.75 ± 0.50*	1.72 ± 0.35*
	20	2.04 ± 0.38*	1.58 ± 0.38*	1.73 ± 0.40*	1.38 ± 0.60*
	40	2.31 ± 0.15*	1.47 ± 0.25*	1.91 ± 0.36*	1.38 ± 0.23*

Subject C	Force, F_d [N]	Distance, l [cm]			
		80	85	90	95
Stiffness [N/m]	0	8907.9 ± 1758.5*	5276.4 ± 517.7*	4584.8 ± 473.9*	4383.6 ± 348.6
	20	7093.8 ± 392.3*	4768.1 ± 289.9*	4086.7 ± 198.1	4066.8 ± 284.7
	40	6159.7 ± 329.0*	5148.8 ± 490.6*	4478.4 ± 320.9*	4215.8 ± 586.5*
Viscosity [Ns/m]	0	115.99 ± 17.90	87.82 ± 5.34*	108.16 ± 6.56	133.10 ± 8.30
	20	113.03 ± 8.38*	89.42 ± 15.15	105.27 ± 5.19	148.45 ± 20.29
	40	124.50 ± 5.69*	123.22 ± 8.91	155.00 ± 12.51	217.93 ± 21.29*
Inertia [kg]	0	1.80 ± 0.10*	1.86 ± 0.20*	1.97 ± 0.48*	1.82 ± 0.09*
	20	1.79 ± 0.41*	2.10 ± 0.22*	1.96 ± 0.17*	1.92 ± 0.13*
	40	1.71 ± 0.37*	2.04 ± 0.33*	1.85 ± 0.23*	1.83 ± 0.37*

TABLE II

NATURAL FREQUENCY FOR ALL SUBJECTS UNDER THE TWO
CONDITIONS.

		Subject A	Subject B	Subject C
Condition	I	20.67 ± 2.60	31.84 ± 5.15	30.11 ± 13.13
	II	65.62 ± 9.40	83.47 ± 17.06	55.93 ± 13.93

[rad/s]

presented in the order from left to right. Under Condition I, human stiffness K_e and viscosity B_e increase in proportional to the distance l and the target force F_d while inertia M_e is almost constant. On the other hand, under Condition II, K_e and Me do not have noticeable characteristics according to l and F_d while B_r changes as same as the result obtained in Condition I. It should be noted that K_e becomes much larger and M_e much smaller by contacting the heel with ground while B_r almost same. The same tendencies can be found for all subjects. The results for all subjects are presented in Table I, where an asterisk in the table (b) denotes that there exists a significant difference with 1 % significance level between Condition I and Condition II by one-side t test.

Table II shows the mean value with standard deviation of a natural frequency for the three subjects calculated from a set of the mean values under all conditions. Note that there exists the notable difference in the natural frequency between Condition I and Condition II. This suggests that a human operator should contact his heel with the ground when he executes quick motion by the foot during a task, such as stepping motion.

The above experimental findings indicate that a human adapt dynamic properties of his/her limbs according to leg posture and foot force as well as the contact condition with a task environment.

IV. INTEGRATION OF HUMAN IMPEDANCE INTO A HUMAN-MACHINE SYSTEM

A. Prototype control system

To simplify the discussion, a human-machine system manipulated by the lower extremities is expressed with a spring-mass-damper system as shown in Fig. 7(a). Dynamic properties of the system can be given by

$$(M_e + M_r)\ddot{X}_e(t) + (B_e + B_r)\dot{X}_e(t) + (K_e + K_r)X(t) = F_e(t), \quad (3)$$

where X_e and F_e are the foot position and force, M_r, B_r, and K_r are the robot inertia, viscosity, and stiffness. The problem is how to make a robot utilize human impedance for regulating the robot impedance parameters according to human movements during a task.
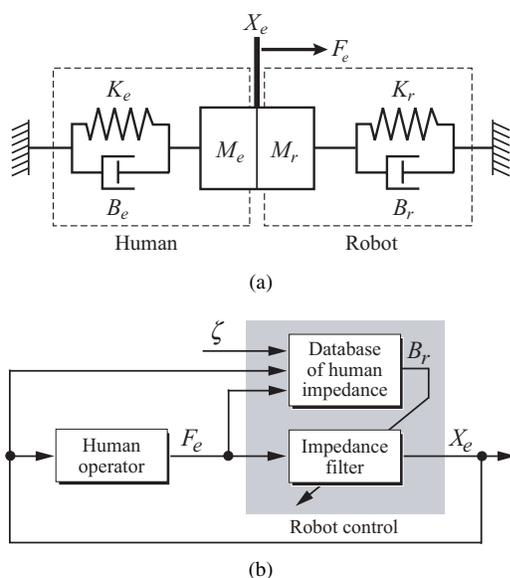
(a)

(b)

Fig. 7. Proposed control structure of a human-machine system using an impedance-controlled robot.

(a) ζ = 0.65

(b) ζ = 1.0

Fig. 8. Robot viscosity depending on human movements for the specified damping coefficient ζ.

As the overall system is a 2nd-order one, in this paper, a prototype control structure is designed as shown in Fig. 7(b). The robot calculates human impedance for the foot position and force from the database of human impedance properties, and has a function of adapting robot viscosity to realize the specified damping coefficient of the overall system ζ with the fixed robot inertia and stiffness depending on the estimated human impedance parameters:

$$\zeta = \frac{B_e + B_r}{2\sqrt{(M_e + M_r)(K_e + K_r)}}. \tag{4}$$

It is expected that the task performance can be improved when the appropriate damping coefficient ζ is designed for a target task.

B. Operational experiments

Basic tests were carried out to examine the designed control structure by using the developed experimental system. A subject was out of the three subjects participated in the impedance measurements.

The subject was instructed to quickly move the step attached at the moving part of the robot with the target distance X_d by his right foot under Condition I (See Fig. 3) according to the visual feedback display, where the initial distance between the hip joint and the step was at $l = 85$ [m]. On the display, the current position of the step (the foot) X_e was always presented with a blue box while the target position X_d was with a red box after the beep sound. Robot viscosity B_r automatically changes in the foot position X_e and force F_e applied by the subject under the specified damping coefficient ζ. The damping coefficient was settled as $\zeta = 0.65$ in Case 1, $\zeta = 1.0$ in Case 2, and $\zeta = 0.65$ $+0.35(X_e/X_d)$ in Case 3. The other experimental parameters were set as $X_d = 4$ [m], $M_r = 2.0$ [kg], and $K_r = 500$ [N/m]
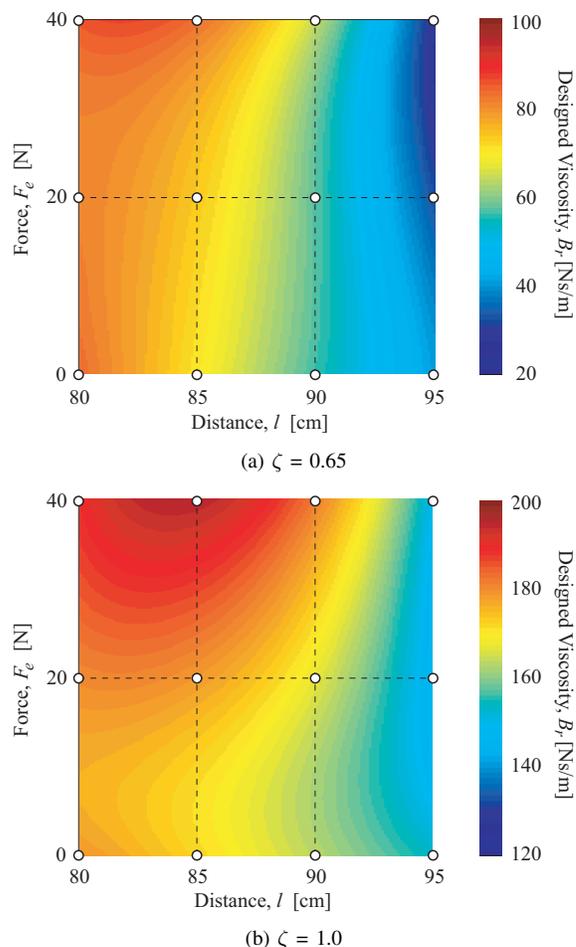
with considerations of the performance of the utilized robotic device, and the number of trials was ten in each case.

Fig. 8 shows the variations of robot viscosity B_r for Case 1 and Case 2 computed by Eq. (4) with the values of human impedance parameters measured at Condition I (a white circle). It can be found that B_r changes depending on the distance (leg posture) l and foot force F_e.

Fig. 9 shows typical time histories of the foot velocity $\dot{X}_e$, the force F_e, and the robot viscosity B_r during the target task for all cases in the order from the top. The designed control structure stably performs with regulating robot viscosity during human movements. It can be seen that the subject generates a single-peaked velocity profile in Case 3 (a blue line). On the other hand, Fig. 10 shows the mean values of the first time when the foot velocity becomes zero after starting the motion, t_v, and the absolute positional error, $E = |X_d - X_e(t_v)|$, with the standard deviation for the last five trials. It can be said that the subject can quickly move the step to the target position in Case 1 while he can accurately do in Case 3. These results demonstrate that both human motion and task performance are influenced by the specified damping coefficient ζ.
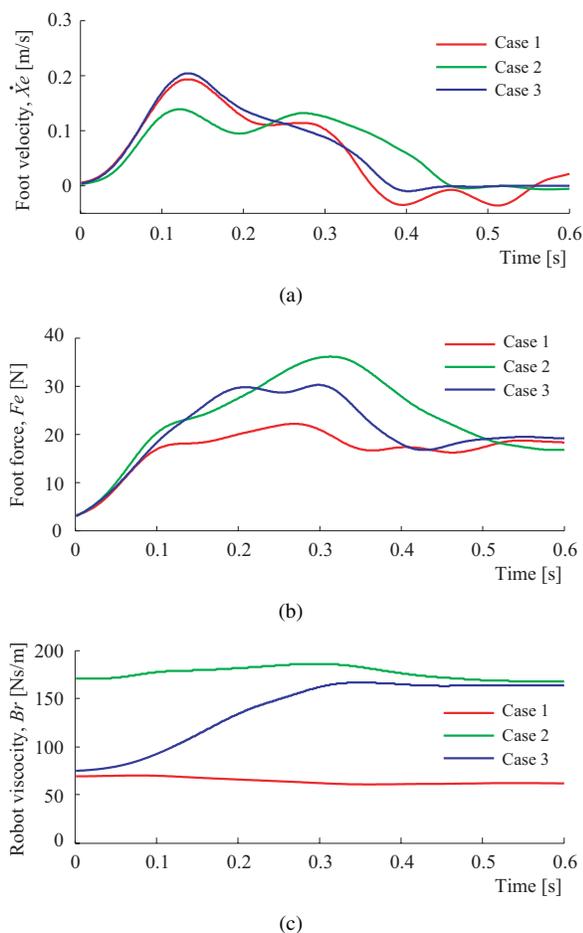
(a)

(b)

Fig. 9.   Typical time histories of human motion and robot viscosity.

(a)

(b)

Fig. 10.   Evaluation results of the subject's movements.

The presented approach could be one of an effective method for integrating human motor characteristics expressed with mechanical impedance into human-machine systems, although there has still exist the problem how to evaluate operational performance and feeling.

V. CONCLUSIONS

This paper has discussed the integration of human impedance properties into a human-machine system composed of the variable impedance-controlled robot.

Focusing a human-machine interface system manipulated by the lower extremities, human leg impedance properties during maintained leg posture were investigated according to the leg posture and foot force. Next a set of basic tests was carried out to evaluate the designed control structure with the database of the measured human impedance by using the developed experimental device.

In the future research, further experiments would be carried out to make a reliable database of human leg impedance. We also plan to apply the presented methodology into other human-machine systems with examining the control structure.
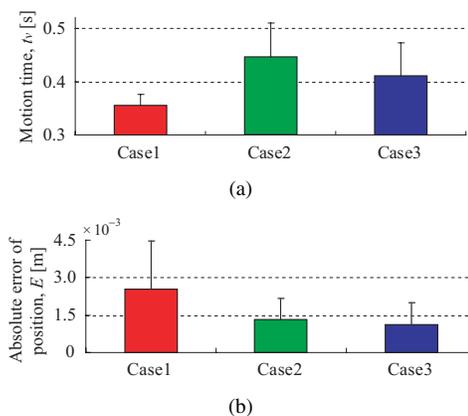
REFERENCES

[1] Y. Tanaka, N. Yamada, I. Masamori, and T. Tsuji: "Manipulability analysis of lower extremities based on human joint-torque characteristics," in Proceedings of the 2nd International Symposium on Measurement, Analysis and Modeling of Human Functions, pp. 261–266, 2004.
[2] Y. Tanaka, N. Yamada, K. Nishikawa, I. Masamori, and T. Tsuji: "Manipulability analysis of human arm movements during the operation of a variable-impedance controlled robot," Proceedings of the 2005 IEEE/RSJ International Conference on Intelligent Robotics and Systems, pp. 3543–3548, 2005.
[3] F. A. Mussa-Ivaldi, N. Hogan, and E. Bizzi: "Neural, mechanical and geometric factors subserving arm in humans," Journal of Neuroscience, vol.5, no. 10, pp. 2732–2743, 1985.
[4] J. M. Dolan, M. B. Friendman, and M. L. Nagarka: "Dynamics and Loaded Impedance Components in The Maintenance of Human Arm Posture," IEEE Transaction on Systems, Man, and Cybernetics, vol.23, no. 3, pp. 698–709, 1993.
[5] T. Tsuji, P. G. Morasso, K. Goto and K. Ito: "Human hand impedance characteristics during maintained posture," Biological Cybernetics, vol. 72, pp. 457–485, 1995.
[6] T. Tsuji and M. Kaneko: "Estimation and modeling of human hand impedance during isometric muscle contraction," in Proceedings of the ASME Dynamic Systems and Control Division, DSC-vol. 58, pp. 575–582, 1996.
[7] S. Park and T. B. Sheridan: "Enhanced human-machine interface in braking," IEEE Transactions on Systems, Man, and Cybernetics-Part A: systems and humans, vol. 34, pp. 615–629, 2004.
[8] N. Hogan: "Impedance control: an approach to manipulation: Parts I, II, III," ASME Journal of Dynamic Systems, Measurement, and Control, vol. 107, no. 1, pp. 1–24, 1985.
[9] H.Kazerooni: "Human-robot interaction via the transfer of power and information signals," IEEE Transactions on Systems, Man, and Cybernetics, Vol. 20, No. 2, pp. 450–463, 1990.
[10] J.E.Colgate: "Robust impedance shaping telemanipulation," IEEE Transactions on Robotics and Automation, Vol. 9, No. 4, pp. 374–384, 1993.
[11] R.Ikeura, and H.Inooka: "Variable impedance control of a robot for cooperation with a human," in Proceedings of the IEEE International Conference on Robotics and Automation, pp. 3097–3102, 1995.
[12] O. M. Al-Jarrah, and Y. F. Zheng: "Arm-manipulator coordination for load sharing using compliant control," in Proceedings of the IEEE International Conference on Robotics and Automation, pp. 1000–1005, 1996.
[13] K.Kosuge, and N.Kazamura: "Control of a robot handling an object in cooperation with a human," in Proceedings of the IEEE International Workshop on Robot and Human Communication, No. 1, pp. 142–147, 1997.
[14] T. Tsumugiwa, R. Yokogawa, and K. Hara: "Variable impedance control based on estimation of human arm stiffness for human-robot cooperative calligraphic task," in Proceedings of the IEEE International Conference on Robotics and Automation, pp. 644–650, 2002.